Groundwater

Thermal Imagery of Groundwater Seeps: Possibilities and Limitations

by Erin Mundy[1], Tom Gleeson[2], Mark Roberts[1], Michel Baraer[3], and Jeffrey M. McKenzie[4]

Abstract

Quantifying groundwater flow at seepage faces is crucial because seepage faces influence the hydroecology and water budgets of watersheds, lakes, rivers and oceans, and because measuring groundwater fluxes directly in aquifers is extremely difficult. Seepage faces provide a direct and measurable groundwater flux but there is no existing method to quantitatively image groundwater processes at this boundary. Our objective is to determine the possibilities and limitations of thermal imagery in quantifying groundwater discharge from discrete seeps. We developed a conceptual model of temperature below discrete seeps, observed 20 seeps spectacularly exposed in three dimensions at an unused limestone quarry and conducted field experiments to examine the role of diurnal changes and rock face heterogeneity on thermal imagery. The conceptual model suggests that convective air-water heat exchange driven by temperature differences is the dominant heat transfer mechanism. Thermal imagery is effective at locating and characterizing the flux of groundwater seeps. Areas of active groundwater flow and ice growth can be identified from thermal images in the winter, and seepage rates can be differentiated in the summer. However, the application of thermal imagery is limited by diverse factors including technical issues of image acquisition, diurnal changes in radiation and temperature, and rock face heterogeneity. Groundwater discharge rates could not be directly quantified from thermal imagery using our observations but our conceptual model and experiments suggest that thermal imagery could quantify groundwater discharge when there are large temperature differences, simple cliff faces, non-freezing conditions, and no solar radiation.

Introduction

Temperature has long been recognized as a useful hydrologic tracer, which can detect stream-aquifer interaction, identify hydrologic thermal heterogeneity and refugia, and delineate flow through fractures (Anderson 2005). Groundwater has an identifiable thermal signature, due to its relatively constant temperature throughout the year, as compared with surface water or land surfaces, which vary on diurnal and seasonal cycles (Anderson 2005; Deitchman and Loheide 2009). At higher latitudes, groundwater temperature is relatively cool compared with air temperature in the summer, and relatively warm in the winter. Recently, there has been a renewed interest in using thermal imagery as a hydrologic tracer motivated by the expanding understanding of the role of temperature in ecohydrology and the development of low-cost temperature-sensing equipment (Anderson 2005; Loheide and Gorelick 2006; Waldick and Conant 2006; Deitchman and Loheide 2009; Pfister et al. 2010; Pandey et al. 2013; Dugdale et al. 2015; Kurylyk et al. 2015; Briggs et al. 2016).

Recent studies have focused on using thermal imagery to detect groundwater springs and qualitatively characterize seepage faces (Loheide and Gorelick 2006; Waldick and Conant 2006). For example, Pfister et al. (2010) used ground-based thermal imagery to identify the location and connectivity of variably saturated areas in a hillslope-riparian-stream system. Deitchman and Loheide (2009) demonstrated that thermal imagery could be used to locate the position of the water table of a stream bank seepage face, as well as distinguish between areas of low, moderate, and high groundwater discharge at the seepage face boundary. In addition, Deitchman and Loheide (2009) observed that thermal imagery provided insight to the differences between diffuse and focused groundwater flow, demonstrating that groundwater flow is more

[1]Department of Civil Engineering, McGill University, Macdonald Engineering Building, 817 Sherbrooke Street West, Room 492, Montréal, Québec H3A 0C3, Canada.

[2]Corresponding author: Department of Civil Engineering and School of Earth and Ocean Sciences, University of Victoria, P.O. Box 3055, EOW 206, 3800 Finnerty Road, Victoria, British Columbia V8P 5C2, Canada; tgleeson@uvic.ca

[3]Département de génie de la construction, École de technologie supérieure, 1100 rue Notre-Dame Ouest, Montréal, Quebec H3C 1K3, Canada.

[4]Department of Earth and Planetary Sciences, McGill University, 3450 University Street, Montreal, Quebec H3A 0E8, Canada.

Article impact Statement: Thermal imagery can locate seeps and differentiate seepage rates but direct seepage quantification is limited by diverse technical factors.

Received January 2016, accepted July 2016.

doi: 10.1111/gwat.12451

discrete and heterogeneous than commonly modelled. In addition to field studies, thermal imagery has also been used in laboratory experiments to quantify groundwater discharge. Pandey et al. (2013) demonstrated that thermal infrared imagery could be used to predict groundwater seepage under highly simplified conditions in a cold room laboratory. Inspired by these results, herein we examine if thermal imagery can be used to quantify groundwater seepage in more realistic and diverse field conditions using observations and experiments.

Groundwater flows out of the subsurface, known as "seepage," when the pressure head is zero at an external boundary in a saturated zone (Boufadel et al. 1999). Seepage faces influence the hydroecology (Dugdale et al. 2015; Kurylyk et al. 2015) and water budgets of lakes, rivers, and oceans and are common along cliff faces, hill slopes, and stream banks. Seepage faces are characteristic of shallow, unconfined groundwater systems, but are seldom included in groundwater modelling (Simpson et al. 2003). This is because at the aquifer scale ($>10\,km^2$), seepage faces make up a small percentage of the modeling domain and their influence on the overall water balance is assumed to be negligible (Romanoa et al. 1999). More recent modelling approaches account for seepage faces by coupling surface water processes directly to groundwater (e.g., Brunner et al. 2009), or specific seepage algorithms (Batelaan and De Smedt, 2005). In riparian zones, the influence of seepage faces on hydrologic and ecologic processes is underestimated by current methods of quantifying seepage face groundwater flux; improved measurement methods are required to describe the interaction between groundwater and these important ecological niches (Deitchman and Loheide 2009).

Our objective is to determine the possibilities and limitations of thermal imagery in quantifying groundwater discharge from discrete seeps. Specifically, the efficacy of thermal imagery for quantifying groundwater discharge in fractured rock is evaluated. The conditions under which thermal imagery are useful, including geology, time of day, sun exposure, and season, are evaluated and discussed. We focus on seepage from discrete point sources, rather than diffuse seepage from a seepage face (Deitchman and Loheide 2009) or semi-diffuse seepage from macropores (Briggs et al. 2016). And we focus on seepage from aquifers with a residence time long enough so that the outflow temperature can be assumed to be close to the mean annual air temperature (suggesting our results may not be applicable to karst and other hydrogeologic systems with short residence times).

Conceptual Model of Temperature Change Below Discrete Groundwater Seeps

Our analysis is motivated by the hypothesis that groundwater discharging from discrete seepage flows as a falling film over the outcrop face (Somasundaran 2006). Falling films, thin water films driven by gravity, are complex systems that can be described using simplified steady-state models such as proposed by Nusselt (1916). At high Reynolds numbers (turbulent flow) falling films are characterised by the presence of waves (Dietze 2010). While waves can enhance heat transfer (Lyu and Mudawar 1991; Groß et al. 2005), they do not affect the heat transfer mechanisms and can be simulated with a simplified steady-state model suitable for identifying the dominant heat transfer factors.

We use a steady-state falling film model to simulate the thermal evolution of water from groundwater that discharges from rock fractures. We consider the simplest scenario that can be observed in natural field conditions: only sensible heat exchange, negligible incoming solar radiation, negligible long-wave radiation, steady-state flow, and steady-state heat exchange within the system (Figure 1). Those conditions are met, for example, during nighttime in the summer with stable and humid atmospheric conditions. The model is applied between two elevations (levels): 0 and n. "0" represents the position situated just below the seepage origin (fracture) and "n" is the position where the water has almost reached the air temperature. In typical summer conditions, water flows out of the fracture at a temperature $T^{\circ}\text{water}_0$, which is colder than the air temperature, $T^{\circ}\text{air}$. Because perennial seepage is primarily targeted in this study, we assume that groundwater residence time is sufficient for $T^{\circ}\text{water}_0$ and the internal rock temperature to be similar to the yearly average air temperature (Anderson 2005). In falling films, convection is the predominant mode of heat transfer, as opposed to conduction (Schröder et al. 1979). In our steady-state falling film model, heat transfer exchange between the air and water primarily occurs via convection, q_A. The heat exchanges within the water film itself, within the rock, across the rock/water interface behind the film (q_R), and at the film margins (q_L) are primarily conductive. Under these conditions, heat exchange is greatest at level 0 where there are the largest temperature gradients between the air/dry rock and the water are observed. At the 0 level, q_{A0} dominates the heat fluxes as it is convective. At level n, the situation differs as the air-water temperature gradient is very low. Heat exchanges at n are therefore of lower intensity than in 0.

This conceptual model suggests that the vertical temperature gradient measured at the center of the water film is mainly a function the convective heat exchange with air (q_A). Therefore, in conditions where different seeps are subject to similar environmental conditions, the vertical temperature gradient is then a function of the seep flow rate. Similarly, if a seep has constant discharge during a period of changing air temperature, the vertical temperature gradient should co-vary with the air temperature.

For the steady-state falling film model, there are many important assumptions. We assume that the effect of latent heat of vaporisation is not a major influence as evaporation should occur equally over the entire water film surface. The difference between the level 0 and level n temperatures will not lead to major changes in evaporative conditions. The latent heat assumption is not valid for the latent heat of fusion, which will occur in

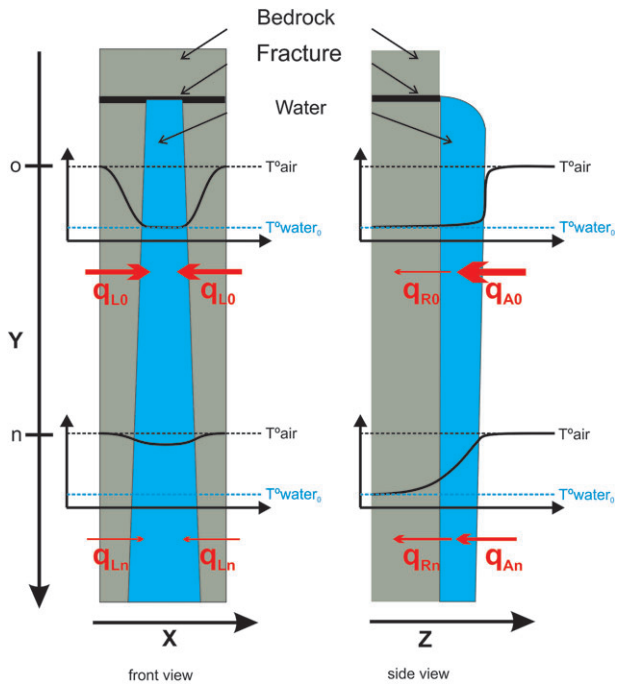

Figure 1. The conceptual model of seepage temperature changes with elevation. Water (in blue) flows along the *y*-axis between elevation 0 and *n*. At elevation 0 and *n*, schematic temperature graphs illustrate the temperature profile along the *x*-axis (left) for photographs looking directly at the cliff face and *z*-axis (right) as a vertical cross-section. On this diagrams T°air represents the air temperature and $T^{\circ}water_0$ the water temperature at the fracture. Red arrows symbolize the heat flux with line thickness illustrating the expected heat flux intensity. This conceptual model is not at a given scale so proportions between features are not respected.

freezing conditions at a given area of the ice and therefore considerably affects the observed cooling process (Pandey et al. 2013). Direct solar radiation is not considered in the steady-state falling film model, although the rock skin may become hotter than the air temperature under these conditions. These assumption may limit the applicability of our model to certain field conditions. In particular, the steady-state falling film model is best applied in non-freezing conditions without direct solar radiation.

For falling films, higher flow rates result in a thicker film and higher average water velocity but do not affect substantially the water-air contact area (Fulford 1964). Higher film thickness and velocity both result in lower heat loss per unit volume, which will be observed as less warming in the summer (or cooling in the winter) as the groundwater seepage travels down a rock face. Therefore the change in seepage temperature with vertical distance from the seep origin, herein called the vertical temperature gradient, should be a function of the discharge rate. A low-vertical temperature gradient corresponds to a small change in temperature with vertical distance down the cliff face, whereas a high-vertical temperature gradient refers to significant changes in temperature with vertical distance. As thermal imagery is able to capture relative temperature of thin film skin (Lel et al. 2008; Peng et al. 2012; Pandey et al. 2013), flow rate differences can be calculated by the use of a thermal IR camera.

Field Area

We test the use of an IR camera to measure seepage flow rates at an unused quarry located in Saint Dominique, Quebec, Canada (Figure 2). This site was chosen because of the large number of groundwater seeps at the site and because of the structure of the quarry itself, with four sides that experience varying levels of sunlight and three elevation levels representing distinct depths beneath the surface. Initial analysis of the field site showed no obvious correlation between seepage flow rate and location, and no clustering of seeps at a specific elevation level or side of the quarry, thereby allowing us to consider the effect of sun exposure on the observed thermal gradients. The climate has a high seasonality (mean January temperature: $-10.2\,^{\circ}$C; mean July temperature: $20.6\,^{\circ}$C), making the quarry an appropriate location to examine the evolution of groundwater seeps in different seasons using thermal imagery. The geology of the quarry consists of Middle Ordovician limestone with thin beds of shale. The rocks were faulted and folded by a single thin-skinned deformation phase of the Paleozoic Taconian orogeny, which involved multiple phases of cross-cutting faults and folds. Taconian structures were subsequently deformed by oblique brittle structures and cross-cut by small and localized volcanic dykes (Séjourné and Malo 2007).

In January 2013, 55 groundwater seeps were identified. Of these, 31 seeps were readily accessible and selected for analysis. Thermal images and physical observations were recorded for 20 of 31 seeps. The remaining 11 seeps had data partially missing because of limited physical access to the seeps, seep absence during some of the field visits, or due to the temporary malfunction of the thermal camera during extreme cold conditions. Herein, each seep is numbered with a two-digit identifier, with the first digit corresponding to the elevation level within the quarry, and the second corresponding to its location on the level, numbered clockwise starting in the north-west corner (Figure 2).

Methods

The applicability of the steady-state falling film model to quantify seeps flow rates was assessed using time-lapse thermal imagery and an artificial seep experiment. Once our understanding of the heat transfer mechanisms were evaluated, winter and summer observations are analysed to assess the potential and limits of this approach in natural field conditions. Thermal and optical images of the groundwater seeps within the quarry were collected during seven field visits between January 2013 and October 2014, capturing the impact of seasons on characterizing groundwater seeps with thermal imagery (Figure 3).

During the winter 2013 and June 2014 field visits, thermal and optical images for each seep were collected

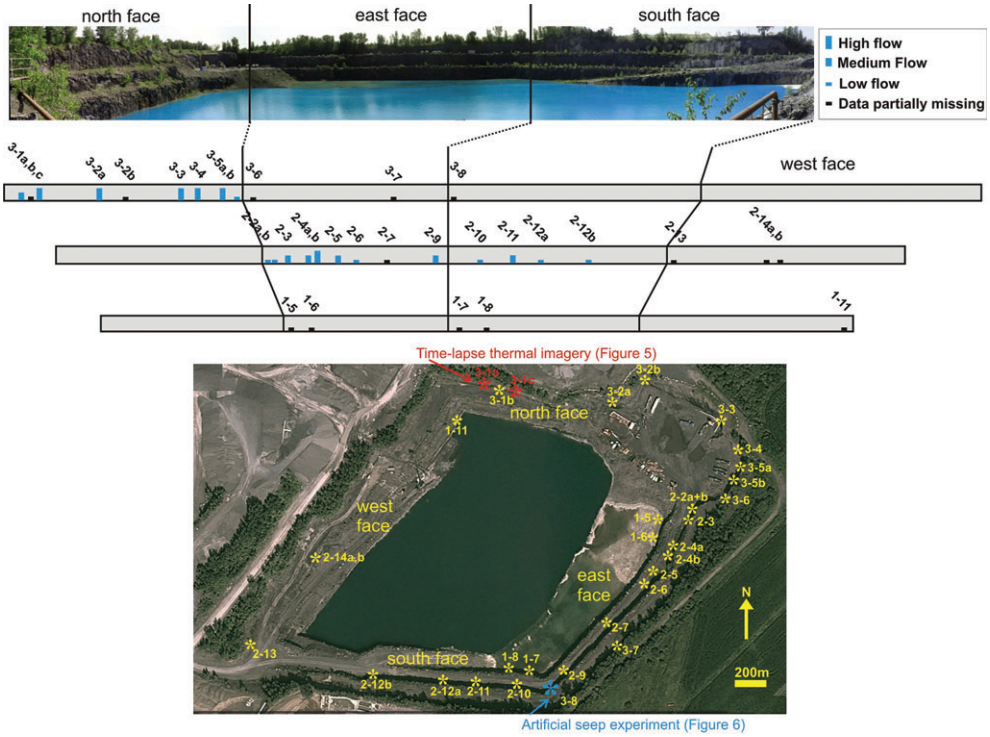

Figure 2. Panoramic photograph of St Dominique quarry with seep locations and categorization of high, medium, or low flow highlighted. Below is aerial photograph of the quarry with the location of the time-lapse thermal imagery and artificial seep experiment indicated.

using a Flir Systems (North Billerica, Massachusetts) B300 thermal IR camera, which measures surface temperature using a 320 × 240 pixel focal plane array and has a spectral range of 7.5-13 µm. The thermal and optical images for each seep during the August, September, and October 2014 field visits were collected using a Jenoptik VarioCam HD thermal IR camera, with a pixel resolution of 768 × 1024 and spectral range of 7.5-14 µm. If only relative temperatures are to be used (as opposed to absolute temperatures), it is not necessary to correct for emissivity, humidity, and observational distance (Schuetz and Weiler 2011). Owing to these benefits of accuracy and analysis, only relative temperatures were used in the thermal image analyses. The distance between the camera and the base of the seepage face was measured, with an accuracy of 0.5 m, to allow the optical images to be plotted to scale; a greater accuracy would have not significantly improved the scaling of the optical images. In addition to the thermal and optical images, physical observations of the seep were also recorded, such as visible flow rate, notable geologic features, and seepage behind the frozen ice seeps.

Time-Lapse Thermal Imagery

A total of 24 h of time-lapse thermal imagery was captured on two seeps in August 2014 to evaluate the role of air temperature and solar radiation, and to estimate the possibility to differential flows intensity. Deitchman and Loheide (2009) showed that time-lapse thermal imagery was useful in determining the optimal time to utilize thermal imagery. In addition, observations over a 24-h period allow for explicit observation of the effects of diurnal solar radiation and the response of the vertical temperature gradient to changes in atmospheric temperature (Figure 2). South-facing seeps 3-1a and 3-1c were chosen for this experiment because they were close to each other and had variable flow rates that were potentially impacted by solar radiation. Thermal and optical images were captured every half hour throughout the duration of the test.

Artificial Seep Experiment

An artificial seep experiment was performed at the quarry in October 2014 to examine the vertical temperature gradient when the discharge rate was known precisely. Two constant head tanks, filled with water (~10 °C), were placed on the third level of the east face of the quarry (Figure 2). This location in the quarry was chosen for its fractured, relatively homogeneous cliff face, with no visible seeps nearby to alter or affect the experiment. Tubing from each head tank was placed onto the cliff face of the second quarry level. Water was discharged from the head tanks at a rate of 1.5 and 5 mL/s, representing medium and high flow rates, respectively. Thermal images of the artificial seeps were collected every half hour for 8 h.

Winter Observations

Three field visits to the quarry were made during the winter of 2013 (January 21, 2013, January 27, 2013, and February 14, 2013). The time of visits was

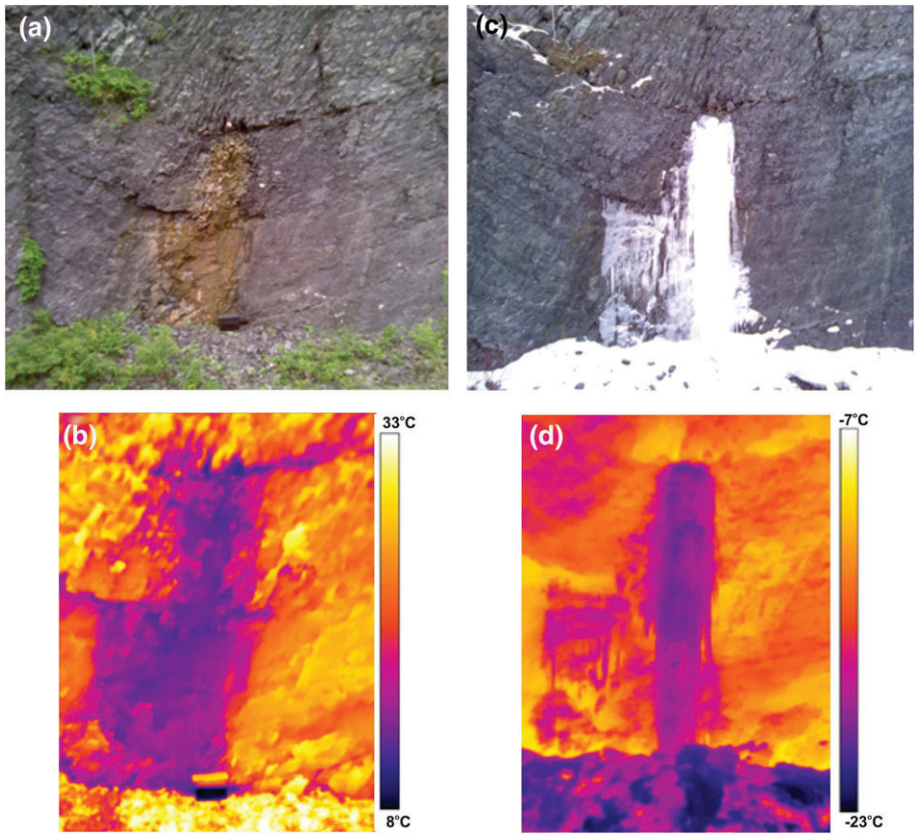

Figure 3. Digital image (a) and thermal image (b) of seep 2-10 taken June 2014. Digital image (c) and thermal image (d) of seep 2-10 taken January 2013.

determined based on local weather forecasts in order to encompass a range of weather conditions (Table S1, Supporting Information). For example, in January 2013, the field visits coincided with a period of prolonged below freezing conditions so that the effect of extreme cold on the development of the ice seeps could be analyzed. Similarly, the field visit in February 2013 took place after a rise in temperature to above freezing, whereby the effect of warmer temperatures on ice seep development could be observed. The seeps identified from these visits were categorized as hydraulically active or inactive. Hydraulically active seeps are those that have at least one area of elevated temperature on a thermal photograph, due to groundwater flowing over an exposed surface, or where physical observations indicate that water is flowing behind the exposed ice surface. The area of elevated temperature on a thermal photograph is henceforth called the active zone. The IR camera only senses the exposed surface, so seeps with groundwater flowing behind the exposed surface cannot be detected using this method (Shea et al. 2012). Seeps are deemed inactive if there is no area of elevated surface temperature on the thermal photograph and no physical observations suggesting flow behind the exposed ice surface.

For the seeps that experienced a period of active groundwater flow throughout the study period, ice formation and degradation was analysed. The optical and thermal images were combined to compare ice growth on optical images and active zones on thermal images. This was completed by resizing and rotating the optical and thermal images from all three trips so as to obtain a consistent scale across all images, which then allowed the percentage change in area of each seep throughout the study period to be calculated (Figure S1, Table S2). This in turn allowed for the flow in each seep to be estimated. The approximate volume of each seep was multiplied by its percentage change in area between January 21, 2013 and January 27, 2013 and ice thickness measured in the field, establishing the volume of ice formed in this 6-d period. Assuming that the ice thickness was uniform across the seep, and that the flow rate was constant, the flow rate in millimeters per second was calculated (Table S2).

Thermal analysis for each active seep utilized ThermaCAM Research Professional software 2.10 to analyze temperature changes in seep temperatures. A multi-point temperature line following the axis of highest temperature (usually vertical but not necessarily) was drawn from the top of the active zone to its base. The relative temperature values were plotted against the percentage change in vertical elevation, using the top of the active zone as a reference value for both axes.

Summer Observations

Three field visits were made during the summer and fall of 2014 (June 11, 2014, August 11, 2014, and September 10, 2014) with cloudy, warm conditions (June

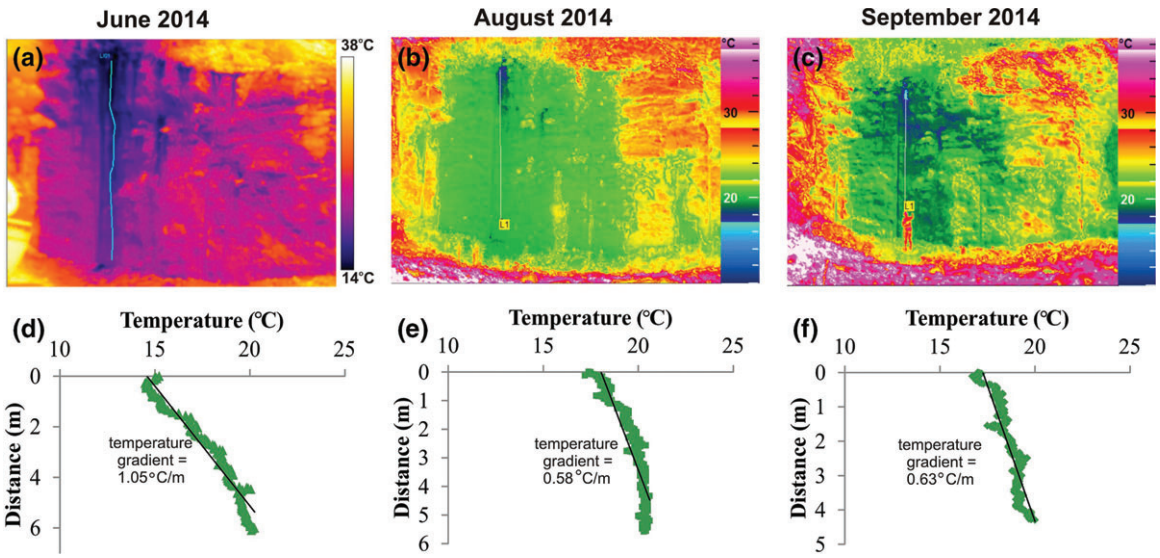

Figure 4. Thermal images and corresponding temperature gradients from June (a, d), August (b, e), and September (c, f) (2014) for seep 3-5. A temperature line profile was recorded down the quarry cliff face using the thermal imaging program which was then plotted against the distance down the cliff face to determine the temperature gradient.

and September,) as well as sunny and hot conditions (August), in order to distinguish the effect warmer temperatures (Table S1). During each visit, the active seeps were categorized as low flow, medium flow, or high flow. The seeps were categorized by physical observations and crude groundwater discharge estimates. Low flow seeps have no visible flow but possess a wet rock face. Medium flow seeps are those with visible flow of approximately 1-4 mL/s, in the form of slow, singular drips. High flow seeps are those with continuous flow greater than 5 mL/s.

Thermal analysis for each seep was completed with a similar method to the active seeps in the winter, using a multi-point temperature line following the axis of lowest temperature (usually vertical but not necessarily) in ThermaCAM Research Professional 2.10 and Jenoptik VarioAnalyzer software. The relative temperature values for each seep plotted against the vertical distance down the seep face are presented in Figure 4. Regression analysis was completed for each seep to develop a function describing the vertical temperature gradient along the cliff face. Fitted lines with R^2 values greater than or equal to 0.8 are considered successful fits. Method performance was assessed by performing Student's two-sample t-tests on vertical temperature gradients of low, medium, and high flows. Tests were conducted at a significance level of 0.05 assuming vertical temperature gradients follow a normal distribution and have unequal variances.

Results

General Observations of Seeps

The location of seep origins, along a well-defined fracture on a bedding plane or at a localized independent fracture intersection, were consistent throughout the study period, but the size, appearance, and thermal profile of the seeps changed over timescales ranging from hours to days. The majority of the groundwater seeps evolved throughout the study period by expanding or sometimes contracting laterally from a singular seep source, originating from a single source in the fractured rock. The apparent hydraulic activity of the seeps decreased in both the winter and summer study period on a weekly time scale, although additional shorter time scale variations may not have been observed due to the times between quarry visits. In winter, there was an observed reduction in the number of active zones identified on the second and third visits. In the summer, the groundwater seepage rates reduced significantly between the June and August visits. A total of 80% of the seeps categorized in June as low flow had no visible flow in August and September. Similarly, 40% of the seeps categorized as medium and high flow in June were reduced to low flow seeps in August and September, correlating to the drier part of the summer.

The location of the active zone on the frozen groundwater seeps did not remain constant throughout the study period. The majority of the active zones were located at the edges of the frozen seeps. This suggests that most frozen seeps predominantly develop laterally across the cliff face as vertical channels, rather than perpendicular to the cliff face (although this must happen too since the frozen seeps are 10–>2 m thick). There was also a clear relationship between zones identified as thermally active and areas of ice growth on the following visit because the thermally active zones were larger and thicker on subsequent visits.

Time-Lapse Thermal Imagery

Time-lapse thermal IR imagery indicates that the vertical temperature gradient and the air temperature are strongly correlated with R^2 of 0.85 and 0.8 for the

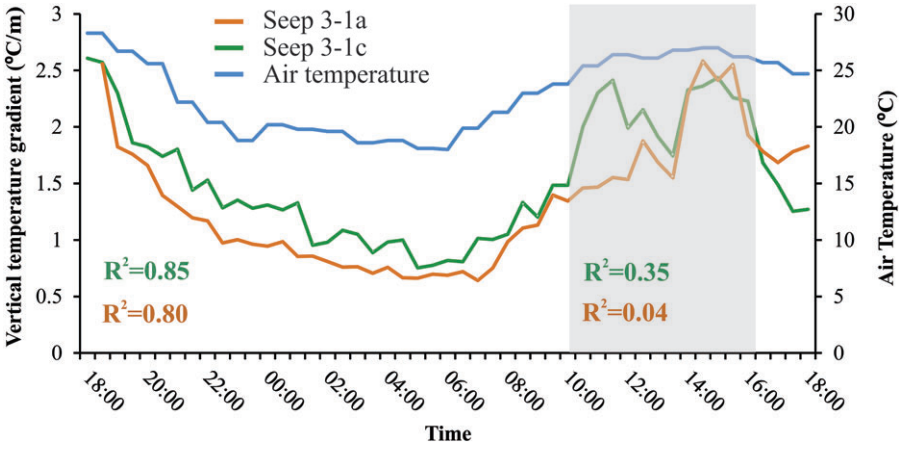

Figure 5. Temperature gradient results from the 24-h time-lapse thermal imagery of seep 3-1a and 3-1c. The shaded area represent the time while the cliff was under direct solar radiations. R^2 values represent the determination coefficient for the air temperature/seep temperature linear regression both for the direct solar radiation free and solar radiation periods.

seeps 3-1c and 3-1a, respectively, for the period of the day when the seeps are not receiving direct solar radiation (Figure 5). The situation is clearly different for the time period when the seeps are receiving direct solar radiations, as the R^2 drops to 0.35 and 0.04 for seeps 3-1c and 3-1a, respectively. Average vertical temperature gradients calculated from Figure 5 are 1.34 °C/m over the direct solar radiation free period for seep 3-1a and 1.06 °C/m for the seep 3-1c. Considering that seep 3-1a exhibit a medium flow rate and seep 3-1c a high flow rate, these results show the capability of the method to qualitatively differentiate between those two flow rate categories. This time-lapse experiment suggests that the steady-state falling film model is reasonable for the simplest possible conditions but that more complex phenomenon drive the vertical temperature gradient under direct solar radiation.

Artificial Seep Experiment

The artificial seep experiment produced vertical temperature gradients slightly larger than the natural groundwater seeps found within the quarry (Figure 6a). The vertical temperature gradients for the medium and high flows were reasonably consistent throughout the experiment, indicating that while the magnitude of the temperature gradients were not as low as expected, they are consistent with qualitative relationship between temperature gradients and seepage flow rates. The vertical temperature gradients may be slightly larger than the natural seeps as the experiment duration was only 8 h, so the artificial seeps may not have had enough time to fully reach steady state. In addition, fractures and small complexities in the cliff face redirected and modified the flow (Figure 6b and 6c). Instead of flowing vertically down the cliff face, the water seeped into the cliff face and flowed horizontally along fractures. This complicated the ability to accurately capture vertical temperature gradients. However, qualitatively, this experiment confirms that higher flows have lower temperature gradients, meaning less appreciable warming down the rock face, as compared to lower flows.

Thermal Analysis – Winter

The relative temperature analysis of the frozen groundwater seeps does not show a clear trend in change in groundwater temperature with distance from top of the active zone. For most seeps, groundwater flow did not cool appreciably along the cliff face (Figure S2). This contrasts with the results of Pandey et al. (2013), where two distinct thermal zones on the active ice surface were observed, with appreciable and consistent cooling with vertical distance from the seep origin.

Winter field conditions deviate significantly from the experimental conditions used in Pandey et al. (2013) as described below, and from those described at the steady-state falling film model that motivates the present research. Among others, winter conditions involve ice as an extra component in the heat exchange budget, latent heat of fusion release, changing surface characteristics in time, and changing flow paths. These conditions make it difficult to achieve more than seep detection during freezing conditions using thermal imagery.

Thermal Analysis – Summer

The relative temperature analysis of the groundwater seeps during the summer study period did show a qualitative relationship between groundwater discharge at the seepage face and rate of groundwater warming down a cliff face (Figure 7). The vertical temperature gradient is generally lower in seeps with higher flow, such as seep 3-5. This relationship suggests that groundwater does not reach equilibrium with the air temperature down the rock face. This can be compared with seep 2-9, a much lower flow, which had a much higher vertical temperature gradient, indicating appreciable warming down the rock face. Student's two sample t-test results show that the three vertical temperature gradient categories have statistically different means, suggesting the proposed method is

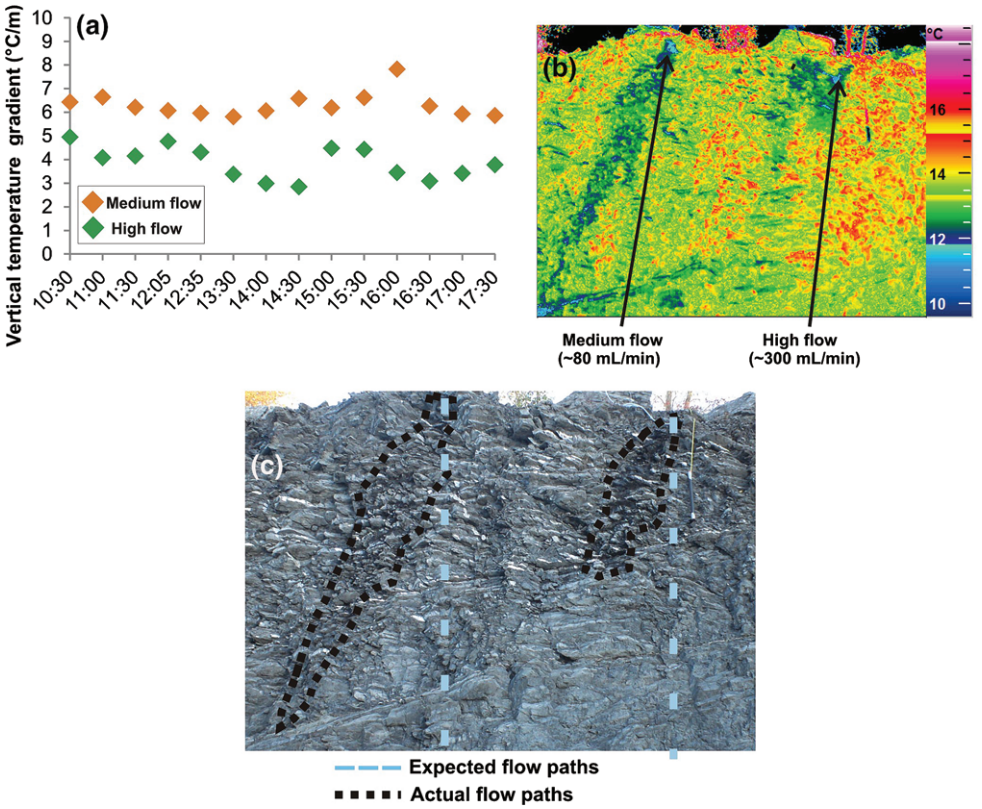

Figure 6. (a) Vertical temperature gradient observed from the artificial seep experiment in October 2014 for medium and high flow. Qualitatively, the medium flow seep has a higher temperature gradient (i.e., gradual warming), as compared with the higher flow seep (i.e., low temperature gradient, less warming). (b) Thermal photograph showing altered flow paths from cliff complexities. (c) Optical photograph showing the geology of the cliff face, with expected and actual flow paths.

able to differentiate between low, medium, and high flows (Figure 7b).

Possibilities for the use of Thermal Imagery of Groundwater Seeps

Locate and Characterize Seeps

Thermal imagery is a non-invasive technique that is effective at locating and qualitatively characterizing groundwater seeps (Loheide and Gorelick 2006; Waldick and Conant 2006; Deitchman and Loheide 2009; Pfister et al. 2010). We add to this growing field of research with a systematic study over one year, using a vertical temperature gradient to qualitatively characterize groundwater seeps. During the winter, thermal imagery can be used to locate areas of active groundwater flow in frozen seeps. In the summer, the time-lapse experiment the artificial seeps experiment confirms the applicability of the simple steady-state falling film model to represent major heat exchange processes in summer shaded or night conditions. Heat exchanges between the environment and the water in our model are driven primarily by the air-water convective process, so the thermal IR imagery is a promising method to characterize seeps under stable conditions. Summertime observations also indicate that thermal imagery can be used to differentiate seepage rates, using the temperature gradient of the water down the vertical cliff face, which is also confirmed with physical observations of flow. Higher flow seeps generally have a lower vertical temperature gradient, meaning less appreciable warming down the cliff face, as compared with lower flows which have a higher vertical temperature gradient. Additionally, thermal imagery is effective at locating low-flow seeps that might have otherwise gone unnoticed. The range in measured vertical temperature gradients for the three different flow rates (Figure 7b) suggest that a more precise flow rate quantification cannot be expected from the method applied in the conditions of this study. If all the summer observations where made when solar radiation was not present, the spreads on Figure 7b may be less.

The results obtained from this study provide direction for future research using thermal imagery to characterize groundwater seepage flux. Detailed discharge measurements, taken at the seep source, should be taken in addition to time-lapse thermal imagery which may help determine a quantitative relationship between groundwater discharge and thermal gradients. This relationship can be further tested by additional artificial "seep" experiments, possibly for longer durations to ensure the artificial seeps achieve steady-state. Finally, observations should focus on times when solar radiation is not present, but when a significant thermal difference between air and water is present.

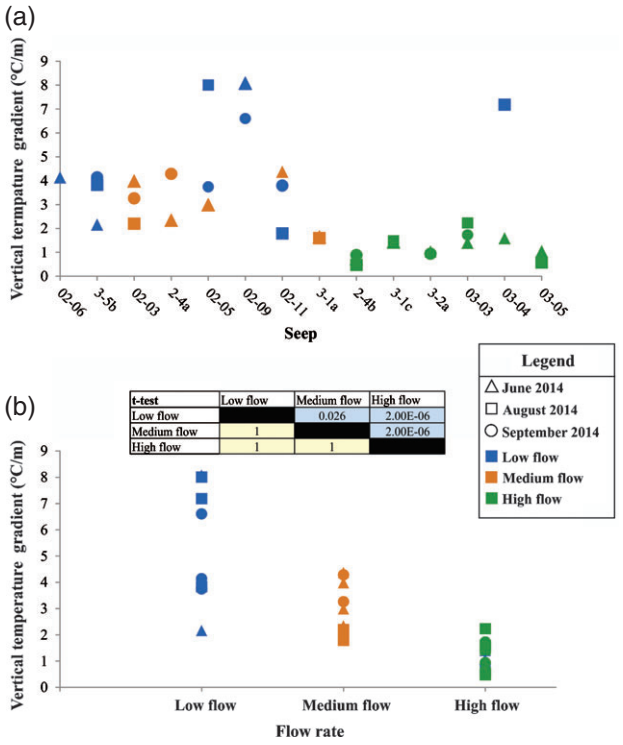

Figure 7. (a) Temperature gradient for all seeps from June to September 2014. (b) Temperature gradient compared to flow rate. The low and medium flow seeps generally have higher temperature gradients (i.e., more warming) as compared with higher flow seeps, which have lower temperature gradients (i.e., less warming). The *t*-test table presents both the hypothesis testing result *h* (yellow cells) and the corresponding p-value (blue cells)

Limitations of the use of Thermal Imagery of Groundwater Seeps

Significant Temperature Differential Between Air and Groundwater Required

Thermal IR imagery is most effective at locating and analyzing seeps when the temperature differential between groundwater and the ambient air temperature is large because air temperature is the primary factor for generating the vertical temperature gradient with stable flow conditions. For example, during the third winter visit, visual observations established that in fact eight seeps remained active but thermal IR imagery identified only one active seep because of a low temperature differential between groundwater and ambient air temperature. The efficacy of thermal IR imagery to locate and characterize seeps is limited to areas with strongly seasonal climates or large-diurnal temperature fluctuations when the air temperature and groundwater temperature are significantly different. For this reason, we did not attempt to make observations during the spring or fall when the temperature differential is not large.

Cliff Face Heterogeneity Affects Thermal Gradients

The artificial seep experiment showed that small complexities in the fractured cliff face topography redirected and modified flow (Figure 6). Robust results require a relatively simple flow path so that the vertical temperature gradient along this flow path can be calculated. The artificial seeps did not flow vertically down the cliff face but instead the water seeped into the cliff face (along the dip of the rocks) and flowed horizontally along fractures. It is possible that the seeps show more warming, and therefore larger temperature gradients, because the water is actually flowing into the rock face (along the dip of the rocks), rather than vertically down the cliff face. Cliff face heterogeneity can also affect natural seeps, as fractured cliff faces are complex and surface flow paths are difficult to predict a priori. This may contribute to the overlap between low, medium, and high flow temperature gradients (Figure 7).

Frozen Seeps Are Complex With No Consistent Thermal Gradients

Frozen seeps observed in the winter were significantly different from the findings of Pandey et al. (2013), where two distinct thermal zones on the active ice surface were observed and there was appreciable cooling along the seepage face. The experiments conducted by Pandey et al. (2013) were in a laboratory (using a simulated rock face made of a metal sheet), which resulted in two distinct thermal zones and consistent cooling along the "seepage face." The thermal conductivity of ice and rocks is much less than the metal sheet. The flat metal sheet roughened with glued sand used in the experiments also greatly differs from the complexity of fractured rocks in the field. In addition, unlike the frozen seeps created by Pandey et al. (2013), the majority of the active zones within the frozen seeps at the quarry were at the edges of seeps. Finally, the seeps simulated in Pandey et al. (2013) were immature, generated on a much smaller time scale than the seeps studied in the quarry. As such, the seeps in Pandey's experimental design may not have had enough time to mature and emulate the nature of the seeps observed in this study. In the field, the lack of a clear trend in temperature change with distance from the top of the active zone suggests that most seeps predominantly develop as vertical channels that migrate laterally across the ice face, and sometimes flow beneath the surface. The lack of observed thermal breaks or gradients in field observations suggest the breakpoint analysis used in Pandey et al. (2013) to determine the two thermal zones was not suitable for the field observations. In conclusion, it seems that even qualitative relationships between discharge rate and vertical temperature gradient are unlikely during freezing conditions, confirming that non-freezing conditions may be more appropriate to focus future efforts on.

Thermal Cameras Have Limitations

It is important to consider the limitations of thermal cameras themselves. In order to obtain quantifiable absolute temperatures from thermal cameras, data must be corrected for emissivity, humidity, and observation distances and known reference temperatures within the images are

required (Aubry-Wake et al. 2015). Changing weather, reflected radiation, and observation angles are a just few of parameters that can affect thermal images. Aubry-Wake et al. (2015) found that changing atmospheric conditions (i.e., overcast, passing clouds) can affect the measured thermal imagery data in high-altitude alpine environments, and are not easily corrected for. Cardenas et al. (2008) noted that radiation emitted from personnel near their area of study resulted in the detection of anomalous sources of radiation in their thermal imagery. Therefore, appropriate framing of the area being captured is important to reduce the amount of reflected radiation. Proper framing must also ensure that the observation angle from the object is less than 45° from the perpendicular, as anything beyond this will affect the emissivity and impacts affect the thermal image (Vollmer and Möllmann 2010). In addition, water surface roughness (wind) and turbidity produces an irregular incident angle, which affects emissivity and can have an effect on the temperature patterns recorded in the thermal image (Liu et al. 1987; Masuda et al. 1988; Hare et al. 2015). A more detailed description of the limitations of thermal imagery can be found in Vollmer and Möllmann (2010). In sum, these complications, if present, must be carefully addressed in order to ensure the thermal signatures captured from a thermal image are correct. Our analysis of thermal images used relative temperature, as it was deemed more accurate than absolute temperatures and avoids the need to correct for emissivity, humidity, and observation distances.

Conclusions

Thermal imagery of groundwater seeps in an unused fractured rock quarry was captured over a 22-month period to determine the efficacy of thermal imagery for quantifying groundwater discharge at seepage faces. The seeps evolved over short periods of time, changing in size, appearance, and thermal profile. Thermal imagery was effective at locating and characterizing seeps. During the winter, areas of active groundwater flow and ice growth can be predicted from thermal images. During the summer, thermal images can be used to qualitatively differentiate between low- and high-flow seeps, using a vertical temperature gradient from the seep source down the vertical cliff face. As predicted by the simplified steady-state falling film model, higher flows will have a lower temperature gradient, suggesting less appreciable warming down the cliff face, as compared with lower flows. This study shows that summer, shade or night in stable conditions are the most favorable the use of thermal imagery in qualitatively differentiating flow rates.

Thermal imagery has several limitations in characterizing groundwater seeps. A robust quantitative relationship between groundwater discharge and the vertical temperature gradient down the vertical cliff face could not be determined using thermal imagery, mainly due to changes in environmental conditions and complexities in the fractured rock cliff topography or ice layers that alter and modify flow paths. Despite the limitations discussed above, thermal imagery is effective at locating and characterizing groundwater flux at the seepage face under certain conditions (no solar radiation, non-freezing, etc.). The results from this study provide insight into the current limitations thermal imagery has in quantifying groundwater discharge at the seepage face, and provides direction on what options to pursue in the future.

Acknowledgments

We thank Jean Dubreuil for access to Les Carrières St-Dominique, Andrea Brookfield and other reviewers and editors for comments that significantly improved this manuscript and fellow McGill students for help in the field, critical review and discussion. Funding for thermal IR equipment was provided by the Canadian Foundation for Innovation and the National Sciences and Engineering Research Council of Canada.

Authors' Note: The authors does not have any conflicts of interest or financial disclosures to report.

Supporting Information

Additional Supporting Information may be found in the online version of this article:

Table S1. Weather conditions during visits to the quarry.
Table S2. Estimates of volumes and flows of ice seeps.
Figure S1. Frozen seep methodology.
Figure S2. Frozen seep results.

References

Anderson, M. 2005. Heat as a ground water tracer. *Groundwater* 43: 951–968.

Aubry-Wake, C., M. Baraer, J.M. McKenzie, B.G. Mark, O. Wigmore, R.Å. Hellström, and L. Lautz. 2015. Measuring glacier surface temperatures with ground-based thermal infrared imaging. *Geophysical Research Letters* 42: 8489–8497. DOI:10.1002/2015GL065321.

Batelaan, O., and F. De Smedt. 2005. Seepage, a new MODFLOW DRAIN Package. *Groundwater* 42, no. 4: 576–588.

Boufadel, M., M. Suidan, A. Venosa, and M. Bowers. 1999. Steady seepage in trenches and dams: Effect of capillary flow. *Journal of Hydraulic Engineering* 125: 286–294.

Briggs, M.A., D.K. Hare, D.F. Boutt, G. Davenport, and J.W. Lane. 2016. Thermal infrared video details multiscale groundwater discharge to surface water through macropores and peat pipes. *Hydrological Processes* 30, no. 14: 2510–2511.

Brunner, P., C.T. Simmons, and P.G. Cook. 2009. Spatial and temporal aspects of the transitions from connection to disconnection between rivers, lakes and groundwater. *Journal of Hydrology* 376: 159–169.

Cardenas, M.B., J.W. Harvey, A.I. Packman, and D.T. Scott. 2008. Ground-based thermography of fluvial systems at low and high discharge reveals potential complex thermal heterogeneity driven by flow variation and bioroughness. *Hydrological Processes* 22: 980–986.

Deitchman, R.S., and S.P. Loheide II. 2009. Ground-based thermal imaging of groundwater flow processes at the seepage face. *Geophysical Research Letters* 36, no. 14: L14401.

Dietze, G.F. 2010. *Flow Separation in Falling Liquid Films,* 345 pp. Göttingen, Germany: RWTH Aachen.

Dugdale, S.J., N.E. Bergeron, and A. St-Hilaire. 2015. Spatial distribution of thermal refuges analysed in relation to riverscape hydromorphology using airborne thermal infrared imagery. *Remote Sensing of Environment* 160: 43–55. DOI:10.1016/j.rse.2014.12.021.

Fulford, G.D. 1964. The flow of liquids in thin films. In *Advances in Chemical Engineering*, Vol. 5, ed. T.B. Drew, J.W. Hoopes, and T. Vermeulen, 151–228. New York: Academic Press.

Groß, S., M. Soemers, A. Mhamdi, F.A. Sibai, A. Reusken, W. Marquardt, and U. Renz. 2005. Identification of boundary heat fluxes in a falling film experiment using high resolution temperature measurements. *International Journal of Heat and Mass Transfer* 48, no. 25–26: 5549–5562.

Hare, D.K., M.A. Briggs, D.O. Rosenberry, D.F. Boutt, and J.W. Lane. 2015. A comparison of thermal infrared to fiber-optic distributed temperature sensing for evaluation of groundwater discharge to surface water. *Journal of Hydrology* 530: 153–166. DOI:10.1016/j.jhydrol.2015.09.059.

Kurylyk, B.L., K.T.B. MacQuarrie, T. Linnansaari, R.A. Cunjak, and R.A. Curry. 2015. Preserving, augmenting, and creating cold-water thermal refugia in rivers: concepts derived from research on the Miramichi River, New Brunswick (Canada). *Ecohydrology* 8, no. 6: 1095–1108.B.

Lel, V.V., A. Kellermann, G. Dietze, R. Kneer, and A.N. Pavlenko. 2008. Investigations of the Marangoni effect on the regular structures in heated wavy liquid films. *Experiments in Fluids* 44, no. 2: 341–354.

Liu, W.-Y., R.T. Gantt, and A. Klemas. 1987. Measurement of the surface emissivity of turbid waters. *Remote Sensing of Environment* 21: 97–109.

Loheide, S.P., and S.M. Gorelick. 2006. Quantifying stream-aquifer interactions through the analysis of remotely sensed thermographic profiles and in situ temperature histories. *Environmental Science & Technology* 40, no. 10: 3336–3341.

Lyu, T.H., and I. Mudawar. 1991. Statistical investigation of the relationship between interfacial waviness and sensible heat transfer to a falling liquid film. *International Journal of Heat and Mass Transfer* 34, no. 6: 1451–1464.

Masuda, K., T. Takashima, and Y. Takayama. 1988. Emissivity of pure and sea waters for the model sea surface in the infrared window regions. *Remote Sensing of Environment* 24: 313–329.

Nusselt, W. 1916. Eine Neue Formel Für den Wärmedurchgang in Kreuzstrom. *Mechanics and Thermodynamics* 1: 417–422.

Pandey, P., T. Gleeson, and M. Baraer. 2013. Toward quantifying discrete groundwater discharge from frozen seepage faces using thermal infrared images. *Geophysical Research Letters* 40: 123–127. DOI:10.1029/2012GL054315.

Peng, J., M.M. Wang, J. Geng, Y.T. Wu, and Z.B. Zhang. 2012. Falling film of ionic liquid-water binary solutions on a uniformly heated vertical wall. *Journal of Heat Transfer* 134, no. 1: 014502–014502-5.

Pfister, L., J.J. McGonnell, C. Hissler, and L. Hoffman. 2010. Ground based thermal imagery as a simple practical tool for mapping saturated area connectivity and dynamics. *Hydrological Processes* 24: 2123–2132.

Romanoa, C.G., E.O. Frind, and D.L. Rudolph. 1999. Significance of unsaturated flow and seepage faces in the simulation of steady-state subsurface flow. *Groundwater* 37: 625–632. DOI:10.1111/j.1745-6584.1999.tb01151.x.

Schröder, J.J., P. Fast, and W. Sander-Beuermann. 1979. Hydrodynamics and heat transfer on vertically finned surfaces in falling film evaporators. *Desalination* 31, no. 1: 19–34.

Schuetz, T., and M. Weiler. 2011. Quantification of localized groundwater inflow into streams using ground-based infrared thermography. *Geophysical Research Letters* 38: L03401.

Shea, C., B. Jamieson, and K.W. Birkeland. 2012. Use of a thermal imager for snow pit temperatures. *The Cryosphere* 6: 287–299.

Simpson, M.J., T.P. Clement, and T.A. Gallop. 2003. Laboratory and numerical investigation of flow and transport near a seepage-face boundary. *Groundwater* 41: 690–700. DOI:10.1111/j.1745-6584.2003.tb02407.x.

Séjourné, S., and M. Malo. 2007. Pre-, syn-, and post-imbrication deformation of carbonate slices along the southern Quebec Appalachian front - implications for hydrocarbon exploration. *Canadian Journal of Earth Sciences* 44, no. 4: 543–564. DOI:10.1139/e06-106.

Somasundaran, P. 2006. *Encyclopedia of Surface and Colloid Science*. New York: Taylor & Francis. 205 pg.

Vollmer, M., and K.-P. Möllmann. 2010. *Fundamentals of Infrared Thermal Imaging, Infrared Thermal Imaging*, 1–72. Weinheim, Germany: Wiley-VCH Verlag GmbH & Co., KGaA.

Waldick, M. K., and B. Conant. 2006. Evaluation of land-based infrared thermography to identify and quantify groundwater discharge to a small stream, paper 13–8, Geological Society of America Annual Meeting and Exposition, 22–25 October, Philadelphia, Pennsylvania.